PNAS RESEARCH ARTICLE | ENVIRONMENTAL SCIENCES SUSTAINABILITY SCIENCE

Effects of climate, land use, and human population change on human–elephant conflict risk in Africa and Asia

Mia Guarnieri[a], Grace Kumaishi[a], Cameryn Brock[b], Mayukh Chatterjee[c], Ezequiel Fabiano[d], Roshni Katrak-Adefowora[a], Ashley Larsen[a], Taylor M. Lockmann[a], and Patrick R. Roehrdanz[b,1]

Edited by Dawn Wright, Esri Inc., Redlands, CA; received July 24, 2023; accepted December 3, 2023

Human–wildlife conflict is an important factor in the modern biodiversity crisis and has negative effects on both humans and wildlife (such as property destruction, injury, or death) that can impede conservation efforts for threatened species. Effectively addressing conflict requires an understanding of where it is likely to occur, particularly as climate change shifts wildlife ranges and human activities globally. Here, we examine how projected shifts in cropland density, human population density, and climatic suitability—three key drivers of human–elephant conflict—will shift conflict pressures for endangered Asian and African elephants to inform conflict management in a changing climate. We find that conflict risk (cropland density and/or human population density moving into the 90th percentile based on current-day values) increases in 2050, with a larger increase under the high-emissions "regional rivalry" SSP3 - RCP 7.0 scenario than the low-emissions "sustainability" SSP1 - RCP 2.6 scenario. We also find a net decrease in climatic suitability for both species along their extended range boundaries, with decreasing suitability most often overlapping increasing conflict risk when both suitability and conflict risk are changing. Our findings suggest that as climate changes, the risk of conflict with Asian and African elephants may shift and increase and managers should proactively mitigate that conflict to preserve these charismatic animals.

human–wildlife conflict | climate change | land use change | biodiversity | species distribution modeling

Significance

Human–wildlife conflict can have detrimental effects on both people and wildlife and can lead to setbacks in conservation efforts. Understanding how conflict risk is likely to shift under a changing climate as agriculture and human populations expand can better allow conservationists and wildlife managers to allocate mitigation and conservation resources for conflict-prone species and regions. To date, little work has been done to anticipate how conflict risk with different species may change in intensity and spatial distribution as human populations expand and climate change impacts intensify. This analysis examines how projected climate change impacts, shifts in agricultural footprint, and changes in human population density may affect the distribution and intensity of conflict with two large, endangered, and conflict-prone species: Asian and African elephants.

Climate change, land use, and human–wildlife conflict are important drivers of the modern biodiversity crisis (1–3). Resource shifts caused by climate change have forced species ranges to shift and contract at unprecedented rates, exacerbating human–wildlife conflict (4–7). Human development and land use further degrades and fragments existing habitat, impacting critical processes such as migration, dispersal, and gene flow (8). As these pressures force humans and wildlife into even closer proximity, there is an increase in shared landscapes and subsequently human–wildlife interactions (9, 10).

Human–wildlife conflict occurs when humans and wildlife interact negatively, resulting in adverse effects such as economic loss, property destruction, and the death or injury of either party (7, 10). Previous studies suggest that negative interactions between humans and wildlife are common in poor and developing regions (11), where communities are dependent on the natural environment for essential resources (12, 13). These negative outcomes from human–wildlife interactions are most prevalent throughout the continents of Asia and Africa, and most reported incidences of human–wildlife conflict in these regions involve large mammals (11). Many conflicts are related to livestock depredation, human deaths and injuries, or crop loss, the last of which is the most frequently reported reason for conflicts worldwide (11, 14, 15). Approximately 20% of the species most frequently involved in human–wildlife conflict are on the International Union for Conservation of Nature (IUCN) Red List (11), including the African savanna elephant (*Loxodonta africana*) and the Asian elephant (*Elephas maximus*), both of which are listed as endangered (16, 17) and are common conflict species (9, 18).

Recently, scholars have sought to model the distribution of human–wildlife conflict as a function of species range, human settlement, and cropland (19) in order to better identify, manage, and mitigate current conflict hotspots. Yet, the future of human–elephant conflict in the face of climate change and continued land use change remains understudied. While present-day distribution of elephants, and therefore current distribution of human–elephant conflict risk zones, is influenced by land use, land cover, and human activities (16, 17, 20, 21), both African and Asian elephants are additionally impacted by climatic shifts, which may exacerbate pressures within existing conflict zones by affecting elephant distribution (16, 17, 22, 23). In addition to climatic shifts, regions including Sri Lanka and Eastern Africa have observed agricultural expansion into important wildlife habitat and migration corridors (24, 25), a process which is expected to continue across Africa and Asia due to

Author contributions: C.B., A.L., and P.R.R. designed research; M.G., G.K., R.K.-A., and T.M.L. performed research; M.G., G.K., R.K.-A., and T.M.L. analyzed data; C.B., M.C., and E.F. reviewed and edited drafts; A.L. and P.R.R. secured funding; reviewed and edited drafts; and M.G. and G.K. wrote the paper.

The authors declare no competing interest.

This article is a PNAS Direct Submission.

[1]To whom correspondence may be addressed. Email: proehrdanz@conservation.org.

This article contains supporting information online at https://www.pnas.org/lookup/suppl/doi:10.1073/pnas.2312569121/-/DCSupplemental.

Published January 29, 2024.

political pressures, food insecurity, and urbanization (23, 26). An understanding of how elephants and people will be impacted by changes in climate and land use is essential to identifying areas where human–elephant conflict may be affected and to developing conflict mitigation strategies that anticipate the shifting landscape of conflict drivers and pressures.

Here, we evaluate areas of potential current and future human–elephant conflict due to changes in land use, human population, and climatic suitability for the Asian elephant and the African savanna elephant over two shared socioeconomic pathways (SSPs) and representative concentration pathways (RCPs). Our objectives are to 1) examine conflict boundaries for the Asian elephant and African savanna elephant under current land use and human population density, 2) explore changes to key conflict drivers within these boundaries under two SSP/RCP scenarios, and 3) identify where changes in elephant climatic suitability overlap with future human–elephant conflict risk zones within existing boundaries.

Results

Baseline Conflict Risk. Following methodology established by Di Minin et al. (19), we define human–elephant conflict risk within extended elephant range boundaries (please see *Materials and Methods*) based on two factors: human population density and cropland density. Using the most recently available data for a present-day baseline, we establish risk cutoffs using the upper decile of present-day population and cropland density within the extended range boundary—the boundary of extant range and adjacent protected areas, as defined by Di Minin et al. (19). Conflict risk levels are split into three classes based on these cutoffs: low, in which neither factor is in the upper decile; medium, in which one of the two factors is in the upper decile; and high, in which both factors are in the upper decile. Under baseline conditions, the majority (78.25%) of the extended range boundary for the African savanna elephant is classified as low conflict risk, 14.3% of the boundary is under medium conflict risk, and 7.45% is identified as high conflict risk. Areas classified as high conflict risk are most concentrated in central East and North Africa (*SI Appendix*, Fig. S1). The Asian elephant extended range boundary is 91.80% low conflict risk, 7.51% medium conflict risk, and 0.69% high conflict risk. Areas identified as high conflict risk are mostly clustered in the southern tip of India, in northeast India, and in Nepal (*SI Appendix*, Fig. S2).

Conflict Risk Change. We completed our analysis for three years: 2030, 2050, and 2070. The trends in conflict risk change remain consistent across years, with greater increasing risk area than decreasing risk area, though the amount of change overall increases from 2030 to 2070 (*SI Appendix*, Tables S4 and S5). We report in-depth results here for the median year, 2050.

African Savanna elephants. Under both the SSP126 and SSP370 scenarios, a large majority of the extended elephant range boundary area (92% in SSP126, the low-emissions sustainability scenario; 82.43% in SSP370, the high-emissions rocky road scenario) does not change conflict risk classification; i.e., neither population nor crop density moves into or out of the upper decile threshold estimated from baseline conditions (Table 1). SSP126 shows scattered areas of increasing conflict risk (6.62% of the boundary area), most concentrated in the northern and central eastern portions of the range (Fig. 1*A*). Areas of decreasing conflict risk are more rare (1.38% of the boundary area) and are scattered throughout the extended range boundary (Fig. 1*A* and Table 1). Overall area of moderate and strong increase in conflict risk under SSP370 is over 2.5 times greater than under SSP126 (16.99% of the boundary area as compared to 6.62%). Area of strong conflict risk increase, where both cropland density and human population density enter the upper decile, is 6.18 times greater under SSP370 than SSP126 (1.05 vs. 0.17% of boundary area) (Table 1). This increase can be seen throughout the extended range boundary (Fig. 1 *A* and *B*). Decreasing conflict risk is uncommon in both scenarios, but there is over twice as much decreasing conflict risk area under SSP126 as SSP370. This difference is most clearly seen in the central eastern and northern portions of the extended African elephant range (Fig. 1 *A* and *B*).

Asian elephants. As with the African elephant, conflict risk does not change within a majority of the extended range boundary under both projection scenarios (94.84% in the low-emissions sustainability scenario SSP126; 91.20% in the high-emissions rocky road scenario SSP370) (Table 1). Under SSP126, areas of increasing conflict risk (4.48% of the boundary area) are scattered throughout the elephant range boundary, but are most concentrated in the western portion of the range, with one small area of strong conflict risk increase (i.e., both cropland and human population density move into the upper decile) in the central east (Fig. 1*C*). Areas of decreasing conflict risk are more rare (0.67% of the boundary area) and are found primarily in the southwestern elephant range area (Fig. 1*C* and Table 1). Under SSP370, conflict risk is increasing across nearly twice as much of the elephant range boundary as under SSP126 (8.33 vs. 4.48%, respectively), and there is 1.4 times less decreasing conflict risk area (0.47 vs. 0.67%) (Table 1). The most concentrated areas of increasing conflict risk in SSP370 are largely the same as in SSP126, but there are also increases in conflict risk within the central- and southeastern portions of the range (Fig. 1*D*). There is one small area of strong conflict risk decrease at the southern tip of India under SSP370. This may be driven by desertification and other climate impacts in southern India pushing rural populations toward cities as subsistence becomes more difficult (27–29).

Conflict Risk Change and Climatic Suitability Change. From species distribution models (SDM) fit for both species using the Maxent algorithm (30, 31), we examined changes in climatic suitability from current conditions along Asian and African elephant extended range boundaries using established cutoffs

Table 1. Percentage of the extended range boundaries for the African savanna elephant (*Loxodonta africana*) and the Asian elephant (*Elephas maximus*) within each conflict change category under SSP126 and SSP370 climate projections in the year 2050

	African elephant		Asian elephant	
Conflict change	SSP 1 - RCP 2.6	SSP 3 - RCP 7.0	SSP 1 - RCP 2.6	SSP 3 - RCP 7.0
Strong decrease	0.00	0.00	0.00	0.02
Moderate decrease	1.38	0.58	0.67	0.45
No change	92.00	82.43	94.84	91.20
Moderate increase	6.45	15.94	4.29	7.83
Strong increase	0.17	1.05	0.19	0.50

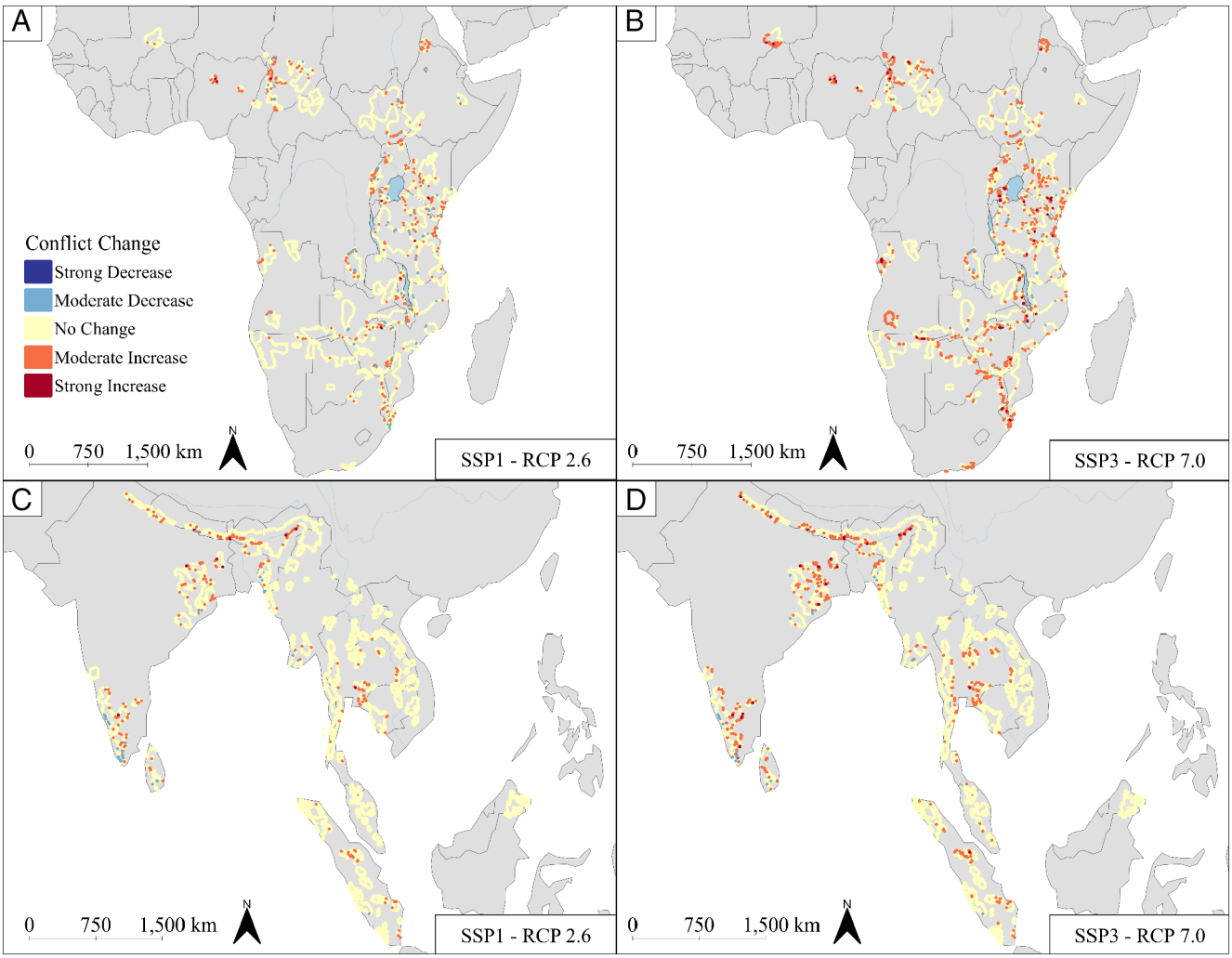

Fig. 1. The change in conflict risk along extended range boundaries for the African savanna elephant (*Loxodonta africana*) and Asian elephant (*Elephas maximus*) under SSP126 and SSP370 climate projections in the year 2050 (*A* – African elephant, SSP126, *B* – African elephant, SSP370, *C* – Asian elephant, SSP126, *D* – Asian elephant, SSP370). Moderate decrease or increase means either cropland density or human population density is moving out of or into the 90th percentile of current-day densities, respectively. Strong decrease or increase means both cropland and human population density are moving out of or into the 90th percentile, respectively. Present-day conflict values can be found in *SI Appendix*, Figs. S1 and S2.

for climatically suitable and unsuitable model values. We created binary maps of climatically suitable or unsuitable habitat using a threshold of the 20th percentile of the model prediction among training presence points for African elephants and 10th percentile training presence for Asian elephants. Areas that are projected to change from one suitability class to another were designated as either decreasing or increasing in suitability according to the direction of change. There is a decrease in cloglog continuous climatic suitability (logistic value of the model mapped over the study domain) across the majority of the extended range boundary for both African and Asian elephants in 2050 across all Global Climate Models (GCMs) in both SSP126 and SSP370, ranging from 67.39 to 89.76% of the range boundary for African elephants and 72.13 to 91.14% of the range boundary for Asian elephants (*SI Appendix*, Tables S6 and S7). This suitability change is corroborated by changes in key climatic variables. Mean annual air temperature (°C) in 2050 increases across 100% of the extended range boundary in all scenarios (all 5 GCMs, SSP126 and SSP370) for African elephants and in all but one scenario (SSP370, GCM MPI-ESM1-2-HR) for Asian elephants—in this case, the increase is across 99.78% of the extended range boundary. Mean daily maximum air temperature of the warmest month (°C) is increasing across 99.35 to 100% of the extended range boundary for African elephants and 89.84 to 100% of the extended range boundary for Asian elephants in 2050. Annual precipitation (kg m^{-2}) is increasing across much of the range boundary for both African (18.80 to 87.96% of the range boundary area, with 7/10 projections over 60%) and Asian elephants (27.20 to 90.08% of the range boundary area, with 8/10 projections over 60%). However, the seasonality of precipitation is also increasing—with the wettest months generally increasing and the driest months decreasing in precipitation. Wettest month precipitation is projected to increase across 47.11 to 91.37% of the Asian elephant range boundary and 38.76 to 88.12% of the African elephant range boundary, while precipitation in the driest month is decreasing within 47.48 to 71.57% of the Asian elephant range boundary. In Africa, driest month precipitation remains unchanged within 46.93 to 54.12% of the elephant range boundary, as these areas already experience no precipitation in the driest month (*SI Appendix*, Tables S8 and S9). Complete information about projected changes in selected bioclimatic variables can be found in *SI Appendix*, Tables S8 and S9. Baseline climatic suitability within the extended range boundary is shown in *SI Appendix*, Figs. S3 and S4. Baseline and projected climatic suitability within the entire region, including the extended range boundary, can be seen in *SI Appendix*, Fig. S5 through *SI Appendix*, Fig. S10.

African Savanna elephants. Climatic suitability for much of the range boundary remains unchanged (i.e., suitability did not move into or out of the upper or lower 10th or 20th percentile) under both SSP126 (low emissions, sustainability) and SSP370 (high emissions, rocky road). There is a net decrease in suitability, however, and areas of decreasing suitability are concentrated in the southwestern portion of the range (Fig. 2 *A* and *B*). A majority of the areas decreasing in suitability are within low conflict risk zones under both projection scenarios, as the majority of the range boundaries are in the low conflict risk class (Table 2). Within areas where conflict risk is changing, decreasing suitability most often overlaps with increasing conflict risk zones (Tables 3). Within areas projected to decline in climatic suitability, the area of increasing conflict risk is 68.3 times larger than the area of decreasing conflict risk under SSP370 and 19 times larger under SSP126 (Table 3). Increasing climatic suitability is much rarer than decreasing suitability in both climate projection scenarios and is more often located in areas of increasing conflict risk, with the difference being more pronounced in the SSP370 scenario (Tables 2 and 3).

Asian elephants. Similarly to African savanna elephants, conflict risk boundaries for the Asian elephant have large regions of stable climatic suitability or no change. Under both projections, there is a net decrease in climatic suitability (Table 2). Areas of decreasing suitability are spread throughout the range but are most concentrated in the central and southeastern range under both projection scenarios. (Fig. 2 *C* and *D*). There is more increasing climatic suitability under SSP370 (high emissions, rocky road) than SSP126 (low emissions, sustainability), and areas of increase are primarily concentrated in the northwestern portion of the range (Table 2 and Fig. 2 *C* and *D*). For areas where risk is changing, a majority of the areas decreasing in suitability are also increasing in conflict risk under both projection scenarios. Within areas projected to decline in climatic suitability, the area of increasing conflict risk is 10.5 times larger than the area of decreasing conflict risk under SSP370 and 3.5 times larger under SSP126 (Table 3). Increasing suitability is much rarer than decreasing suitability in both climate projection scenarios and is located within areas of decreasing conflict risk or no change under SSP126 and primarily within areas of increasing conflict risk under SSP370 (Tables 2 and 3).

Discussion

Our results suggest that climate change and shifts in human population density and crop patterns will likely shift and exacerbate human–wildlife conflict risk with both Asian elephants and African savanna elephants along their current extended range boundaries, and the intensity of this shift is dependent upon the climate change scenario.

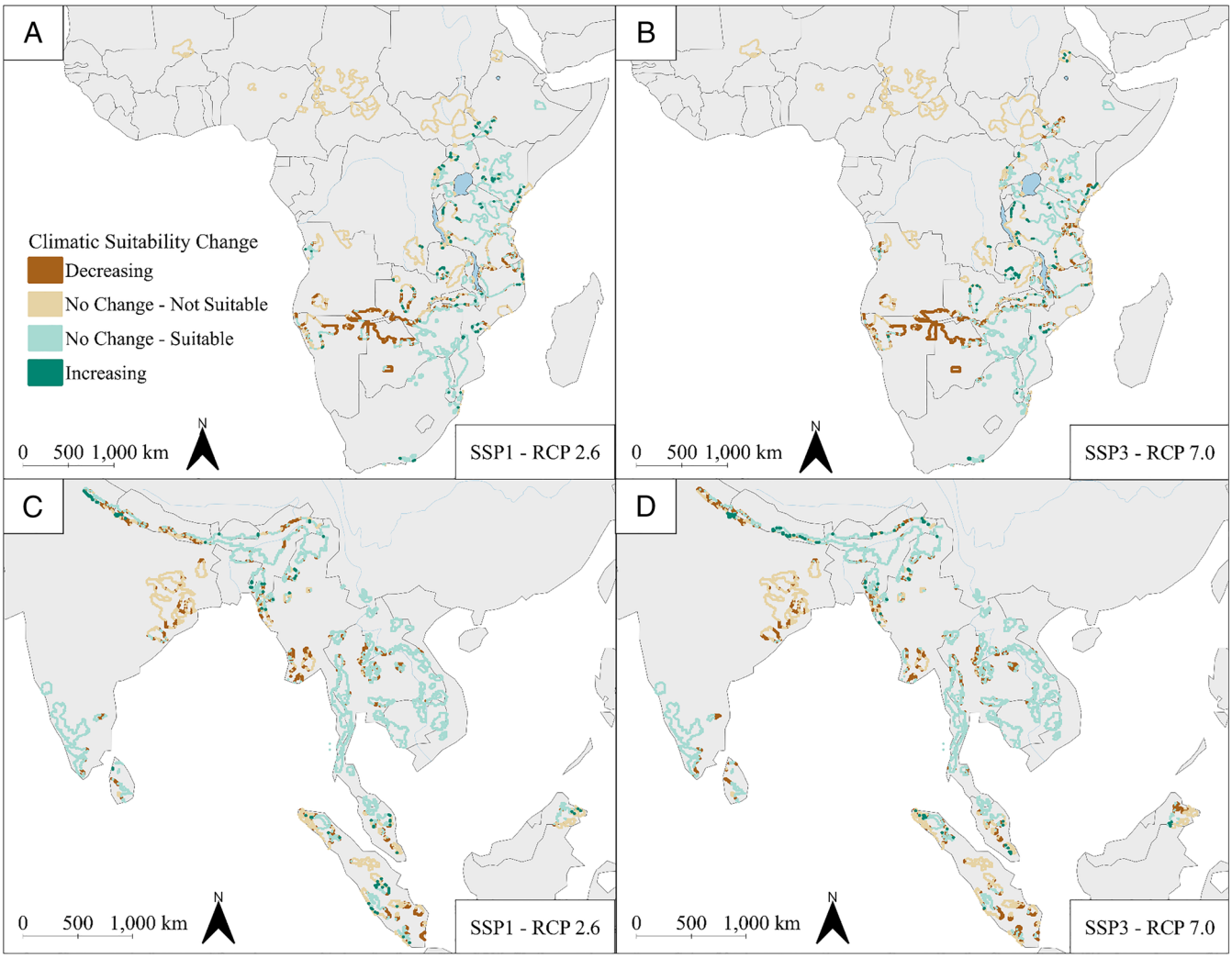

Fig. 2. Change in climatic suitability within the extended range boundary for the African savanna elephant (*Loxodonta africana*) and Asian elephant (*Elephas maximus*) under SSP126 and SSP370 climate projections in the year 2050 (*A* – African elephant, SSP126, *B* – African elephant, SSP370, *C* – Asian elephant, SSP126, *D* – Asian elephant, SSP370). Baseline climatic suitability values can be found in *SI Appendix*, Figs. S3 and S4.

Table 2. The percentage of the extended range boundary area within each climatic suitability change category and conflict risk category for the African savanna elephant (*Loxodonta africana*) and the Asian elephant (*Elephas maximus*) under SSP126 and SSP370 climate projections in the year 2050, under the GFDL-ESM4 GCM

	Conflict risk															
	African elephant								Asian elephant							
	SSP1 - RCP 2.6				SSP3 - RCP 7.0				SSP1 - RCP 2.6				SSP3 - RCP 7.0			
Suitability change	Low	Medium	High	Total	Low	Medium	High	Total	Low	Medium	High	Total	Low	Medium	High	Total
Decreasing suitability	10.47	1	0.18	11.66	11.31	2.41	1.07	14.79	10.21	1	0.17	11.38	8.84	1.61	0.11	10.56
No change—not suitable	33.08	8.36	3.25	44.69	29.19	11.31	4.33	44.82	21.87	2.85	0.54	25.26	20.72	3.11	0.74	24.57
No change—suitable	29.09	6.84	5.11	41.04	23.31	8.09	6.51	37.91	55.26	6.56	0.52	62.34	54.04	8.08	1.04	63.16
Increasing	1.76	0.4	0.45	2.61	1.78	0.42	0.28	2.48	0.93	0.09	0.00	1.02	1.15	0.39	0.17	1.72

The majority of the extended range boundary for both species did not move from one risk category to another in this analysis (i.e., population density and cropland density did not move into or out of the 90th percentile). Paralleling the methods of Di Minin et al. (19), though focusing solely on elephants, we use only the top decile for each risk category, yielding a conservative estimate of spatial conflict risk. Our results are geographically consistent with DiMinin et al.'s analysis on African elephants and with existing conflict analyses for Asian elephants (32–35). Despite a conservative approach, we observe a net increase in conflict risk under both projections, with a greater increase under the high-emissions rocky road scenario (SSP370), suggesting that stronger climate change impacts will lead to a larger increase in conflict risk pressures for African and Asian elephants. SSP370 is characterized by large population growth in developing countries, unlike the low-emissions sustainability scenario (SSP126), which shows low population growth globally (36), and several studies show that human population growth leads to higher instances of conflict (37–39), though the relationship may not be linear (40, 41). SSP370 also predicts large-scale losses of forests and natural lands due to cropland and pasture land expansion, whereas SSP126 predicts much lower expansion of cropland and expansion of forest cover (36, 42). This is consistent with our results, as crop density or area under cultivation is a primary driver of conflict (34, 37, 41, 43, 44).

When examining the overlap of changes in climatic suitability and conflict risk, we found that decreasing suitability most often overlaps increasing conflict risk. There is a net decrease in climatic suitability for both Asian and African elephants in 2050, with a larger decrease under SSP370 for African elephants and surprisingly similar decreases between SSP370 and SSP126 for Asian elephants. Decreasing climatic suitability may have complex implications for conflict risk that vary between regions. For example, several studies suggest that decreasing habitat suitability for Asian elephants will lower conflict risk due to a reduction in elephant numbers (45–47), with a potential for short-term increases in risk due to lag times (46). Research on African elephants is more mixed, with some studies suggesting that conflict decreases with decreasing habitat suitability (19) while others suggest the opposite (47, 48). While this study examines climatic suitability rather than habitat suitability, climatic suitability is a component of habitat suitability and may have similar trends. Future studies linking field observations of conflict with species distribution models, such as the one presented here, could enable a clearer understanding of the implications of reduced climatic suitability on conflict.

There are several caveats to our study. First, following Di Minin et al. (19), we consider total cropland including all crop types. Yet, rice, maize, and wheat are particularly favored by elephants (40, 49–54), and the future distribution of these crops may influence conflict locations. We do not examine seasonality in this analysis as the conflict drivers explored here represent yearly or multi-year means, but conflict with elephants is known to be more common during the rainy season when crops are mature (34, 41, 50, 52, 54–58). Future

Table 3. The percentage of the extended range boundary area within each climatic suitability change category and conflict risk change category for the African savanna elephant (*Loxodonta africana*) and the Asian elephant (*Elephas maximus*) under SSP126 and SSP370 climate projections in the year 2050, under the GFDL-ESM4 GCM

	Conflict risk													
	African elephant						Asian elephant							
	SSP1 - RCP 2.6			SSP3 - RCP 7.0			SSP1 - RCP 2.6			SSP3 - RCP 7.0				
Suitability change	Mod. Dec.	Mod. Inc.	Strong Inc.	Mod. Dec.	Mod. Inc.	Strong Inc.	Mod. Dec.	Mod. Inc.	Strong Inc.	Strong Dec.	Mod. Dec.	Mod. Inc.	Strong Inc.
Decreasing suitability	0.02	0.38	0.00	0.03	1.93	0.12	0.11	0.39	0.00	0.02	0.07	0.93	0.02
No change—not suitable	0.55	3.4	0.05	0.3	7.44	0.2	0.15	1.35	0.09	0.00	0.11	2.09	0.2
No change—suitable	0.77	2.56	0.12	0.25	6.31	0.72	0.37	2.56	0.11	0.00	0.24	4.58	0.26
Increasing	0.05	0.1	0.00	0.00	0.22	0.02	0.04	0.00	0.00	0.00	0.04	0.26	0.02

"No Change" conflict risk categories have been omitted. Abbreviations: Mod. = moderate, Dec. = decrease, Inc. = increase. Columns show the direction of change.

analysis at higher temporal resolution could reveal whether projected conditions may further amplify conflict during certain periods. Occurrence points used to create our climatic suitability models were confined to current range extents for both African and Asian elephants, which may reduce the accuracy of these models (as these species once roamed much larger areas) and exclude some impacts of range shifts due to climate change on the spatial distribution of conflict risk. Further, our use of a 10th or 20th percentile cutoff when classifying suitable versus unsuitable habitat may have obscured areas of moderate climatic suitability. Finally, we assume that increasing human population and cropland density are the primary drivers of conflict. However, a community's response to elephant behaviors will depend on their tolerance for these species, which varies between communities and ethnic groups based on cultural, spiritual, and economic relationships to elephants (59–64). Future studies can build on this work by exploring continuous changes in these and additional risk factors; exploring habitat and climatic suitability on a smaller, regional scale; incorporating more information about local crops, human population density, and tolerance; and accounting for potential future species range shifts and what that means for the spatial distribution of conflict.

As climate change progresses and human populations expand, adapting management strategies to account for shifts in the location and intensity of human–wildlife conflict risk will become increasingly important. By exploring how climate and land use change is likely to alter climatic suitability and conflict risk with African and Asian elephants, we provide valuable insight for management of conflict with these species under a shifting climate regime. In addition to consideration of sociocultural context and regional variations in risk pressures, an understanding of future conflict risk can help managers more effectively plan and implement mitigation strategies to improve coexistence with and conservation of these charismatic and important species.

Materials and Methods

Our analysis was done in two stages. First, we analyzed future conflict risk within existing conflict boundaries following Di Minin et al. (19). Then, we examined projected changes in climatic suitability within these conflict boundaries, and the intersection of suitability and conflict risk changes. A graphical overview of our methods can be seen in *SI Appendix*, Fig. S11.

Conflict Boundaries. Following methodology established by Di Minin et al. (19), we used cropland density and human population density data to examine potential conflict boundaries for the Asian elephant and the African savanna elephant under current and future conditions. Cropland density data for 2015 were from Chen et al. (65) and population density data for 2010 were from the WorldPop database (66). Creating potential conflict boundaries involved three main phases: creating a ranked pressure layer, creating an extended range map, and intersecting the pressure layer with the range map boundary. Di Minin et al. (19) performed their analysis on current-day values. We expanded our analysis by using this methodology to analyze projected conflict risk estimates for two shared socioeconomic pathway (SSP) and representative concentration pathway (RCP) pairings in 2050, as described in O'Neill et al. 2016 (42) and Riahi et al. 2017 (36): SSP1 – RCP 2.6 (Sustainability–Taking the Green Road; low challenges to mitigation and adaptation, low emissions) and SSP3 – RCP 7.0 (Regional Rivalry–A Rocky Road; high challenges to mitigation and adaptation, high emissions). These will henceforth be called SSP126 and SSP370. Projected future cropland density data were from Chen et al. (65) and projected future population density data were from Li et al. (67).

Creation of ranked pressure layers. Population data (67) were projected to match the coordinate reference system and resolution of the land cover data (65). Land cover rasters were reclassified to keep only cropland. Both population density and cropland layers were aggregated by a factor of 10 to align with buffer width and facilitate large-scale analysis (using a sum function for the population data and a mean function for the cropland data) and filtered to keep only the upper decile (90th percentile and above), following the methodology of Di Minin et al. (19). These upper decile layers were converted to binary layers that delineate the upper decile from the bottom 90%. Finally, the binary layers were used to derive a ranked pressure layer, with three classes: low conflict pressure (a pixel was not within the upper decile for cropland or population density); medium conflict pressure (a pixel was within either the upper decile of cropland or population density); and high conflict pressure (a pixel was within the upper decile for both cropland and population density). These thresholds were held constant for both current-day and projected pressure layers, with a cutoff for human population density of 5,184 people per 100 km^2 and a cutoff for cropland density of 65% cropland cover.

Creation of extended range map. Following the methodology of Di Minin et al. (19), and with the understanding that conflict with elephants is often highest around the borders of protected areas (14, 47, 68, 69), we then created an extended range map. Creating the extended range maps required polygons of species ranges obtained from IUCN (16, 17) and polygons of world protected areas obtained from the Protected Planet database (70). IUCN range polygons were filtered to only include extant populations, and protected areas polygons were filtered to keep only the following categories as done by Di Minin et al. (19): Ia (Strict Nature Reserve), Ib (Wilderness Area), II (National Park), III (Natural Monument or Feature), and IV (Habitat/Species Management Area). Protected area polygons which intersected range polygons were merged with the range layer to create one layer for an "extended" range.

Analysis of conflict boundaries. Still following Di Minin et al. (19), we buffered the extended range map by 10 km and kept only the buffer area (from the edge of the extended range polygons to the edge of the 10 km buffer). Buffer polygons were intersected with each ranked pressure raster to show conflict likelihood along extended range boundaries for each scenario. To examine the change in conflict risk under different climate scenarios, we subtracted the baseline conflict boundary raster from each projected raster layer. The resulting rasters were then converted to polygons, with classes from strongly decreasing conflict risk (both population and cropland density moving out of the upper decile) to strongly increasing conflict risk (both population and cropland density moving into the upper decile).

Baseline Climatic Suitability Models.

Obtaining species presence and bioclimatic data. We obtained occurrence data for the African and Asian elephant species from the Global Biodiversity Information Facility (GBIF) using the rgbif package (71), excluding fossils, preserved specimens, and individuals in captivity. We identified three major subspecies of the Asian elephant: the Indian elephant (*Elephas maximus indicus*), the Sri Lankan elephant (*Elephas maximus maximus*), and the Sumatran elephant (*Elephas maximus sumatranus*); we included all subspecies in our models because they are highly ecologically and genetically similar (16, 72, 73). We selected occurrence points that fell within the time period for which our bioclimatic environmental variables were classified (1981 to 2010 for the African elephant, 1981 to 2021 for the Asian elephant due to fewer available data points). We then spatially thinned the occurrence points for the African and Asian elephant species, removing points closer than 10 km to each other to reduce sampling error in the model.

Selection of bioclimatic variables. Bioclimatic variables at a resolution of 30-arcsec were selected from CHELSA Version 2.1 for the year 2010 (74). African elephant variables were based on methodology by Dejene et al. (19), which modeled current and future geographical distributions of the African elephant to assess the impacts of climate change and land cover on the species' distribution. Our initial selection of variables included the following: mean annual temperature (bio1), mean diurnal temperature range (bio2), isothermality (bio3), maximum temperature of warmest month (bio5), annual precipitation (bio12), and precipitation of wettest (bio13) and driest months (bio14). Upon further exploration of these variables, we found that bio14, when projected into the future, was missing large amounts of data in Africa. Thus, we replaced bio14 with the most closely related variable: precipitation of the driest quarter (bio17) (*SI Appendix*, Table S1).

Asian elephant variables were selected based on Asian elephant ecology and existing species distribution models in published literature (18, 46, 75). We narrowed our selection to the following eight variables: mean annual air temperature (bio1), mean diurnal air temperature range (bio2), temperature seasonality (bio4), minimum temperature of the coldest month (bio6), annual temperature

range (bio7), annual precipitation amount (bio12), precipitation of the driest month (bio14), and precipitation seasonality (CV) (bio15) (*SI Appendix*, Table S1).

Baseline climatic suitability. To model baseline African and Asian elephant climatic suitability, we used the Wallace species distribution modeling (SDM) interface (76) and the maxent algorithm (30, 31). We generated 10,000 background points and split the data into training (75%) and test (25%) sets to validate the model. After reviewing AUC values, response curves, and map outputs from model iterations using different regularization multiplier (rm) values for each species, we selected the LQ model with an rm value of 1 for the African elephant (LQ.1 AUC = 0.83, LQ.2 AUC = 0.82) and the LQ model with an rm value of 0.5 for the Asian elephant (LQ.0.5 AUC = 0.78, LQ.1 AUC = 0.77). This decision was further validated by a 2010 paper published by Richmond et al. (77), which found that an rm value of 0.5 produced the highest AUC value for the Asian elephant. To visualize probability of species occurrence on a 0 to 1 scale, we created a map prediction using the cloglog transformation. We produced both continuous climatic suitability maps and binary climatic suitability maps. The binary models for the African and Asian species were created using the 20th and 10th percentile training threshold, respectively, since these thresholds aligned best with the species' current IUCN ranges and the results of their continuous climatic suitability models.

Projected climatic suitability. We projected the African and Asian elephant climatic suitability models using CHELSA variables for the time series 2011–2040, 2041–2070, and 2071–2100 for SSP126 (low emissions, sustainability) and SSP370 (high emissions, rocky road). Each scenario included five general circulation models (GCMs): GFDL-ESM4, IPSL-CM6A-LR, MPI-ESM1-2-HR, MRI-ESM2-0, and UKESM1-0-LL. We display results from GFDL-ESM4 in the main text, following prioritization by the ISIMIP3b protocol (70). Results for additional models are presented in *SI Appendix*, Tables S2 and S3. Results had SD between 0.64 and 6.10 across the five GCMs analyzed. 9.51 to 20.60% of the extended range boundary for African elephants became unsuitable in SSP126, as compared to 13.31 to 22.81% of the extended range boundary in SSP370. 6.49 to 17.22% of the extended range boundary for Asian elephants became unsuitable in SSP126, vs. 8.60 to 24.22% in SSP370 (*SI Appendix*, Tables S2 and S3). Additional exploration into model contribution to climatic suitability model performance revealed that GFDL-ESM4 was most frequently selected as the median of the five models across species and SSP-RCP scenarios.

We created continuous and binary climatic suitability models for each GCM. For binary climatic suitability models, we used the 20th percentile training presence threshold for the African elephant and the 10th percentile training presence threshold for the Asian elephant, in congruence with their respective baseline climatic suitability models. We subtracted the binary baseline model from each binary projected model to visualize where suitability decreased, remained unsuitable, remained suitable, or increased from the baseline to the future time period. These binary maps represent conservative estimates for stage shifts from suitable to unsuitable. We additionally calculated differences between cloglog continuous projected and baseline climatic suitability and differences for select bioclimatic variables (bio1, bio5, bio12, bio13, and bio14).

Data, Materials, and Software Availability. Code repository data have been deposited in Github (https://github.com/gkumaishi/Elephant_HWC) (78). Previously published data were used for this work (16, 17, 65–67, 70, 71, 74).

ACKNOWLEDGMENTS. We acknowledge funding from the NSF (DEB-2042526), the Arnhold Research Fellows program, and the UC Santa Barbara-Conservation International Climate Solutions Collaborative. We thank Dr. Ganesh Pant, Scott Wilson, and Dr. Rosemary Shikangalah for providing expert advice and review. We thank Benitto Ndana, Colgar Sikopo, Peter Venekamp, and Jord Veldkamp for providing input and advice. We thank Maggie Klope, Mika Leslie, and Chris Kracha for providing assistance with literature review and geospatial analysis. Finally, we wish to thank our reviewers for their time and insights.

Author affiliations: [a]Bren School of Environmental Science and Management, University of California, Santa Barbara, CA 93106-5131; [b]Moore Center for Science, Conservation International, Arlington, VA 22202; [c]North of England Zoological Society, Upton, Chester CH2 1LP, United Kingdom; and [d]Department of Wildlife Management and Tourism Studies, University of Namibia, Katima Mulilo 1096, Namibia

1. C. D. Thomas *et al.*, Extinction risk from climate change. *Nature* **427**, 145–148 (2004).
2. T. Newbold *et al.*, Global effects of land use on local terrestrial biodiversity. *Nature* **520**, 45–50 (2015).
3. P. J. Nyhus, Human–wildlife conflict and coexistence. *Annu. Rev. Environ. Resources* **41**, 143–171 (2016).
4. C. Parmesan, G. Yohe, A globally coherent fingerprint of climate change impacts across natural systems. *Nature* **421**, 37–42 (2003).
5. D. Tilman *et al.*, Future threats to biodiversity and pathways to their prevention. *Nature* **546**, 73–81 (2017).
6. J. Bhatt, A. Das, K. Shanker, *Biodiversity and Climate Change: An Indian Perspective* (Ministry of Environment, Forest and Climate Change, Government of India, New Delhi, India, 2018).
7. B. Abrahms, Human-wildlife conflict under climate change. *Science* **373**, 484–485 (2021).
8. K. S. Delaney, S. P. Riley, R. N. Fisher, A rapid, strong, and convergent genetic response to urban habitat fragmentation in four divergent and widespread vertebrates. *PLoS One* **5**, e12767 (2010).
9. S. Anand, S. Radhakrishna, Investigating trends in human-wildlife conflict: Is conflict escalation real or imagined? *J. Asia Pacific Biodiversity* **10**, 154–161 (2017).
10. IUCN, IUCN SSC guidelines on human-wildlife conflict and coexistence (2023). https://doi.org/10.2305/YGIK2927. Accessed 16 May 2023.
11. D. F. Torres, E. S. Oliveira, R. R. Alves, Conflicts between humans and terrestrial vertebrates: A global review. *Trop. Conserv. Sci.* **11**, 1940082918794084 (2018).
12. R. F. Barnes, The conflict between humans and elephants in the Central African forests. *Mammal Rev.* **26**, 67–80 (1996).
13. A. Choudhury, Human–elephant conflicts in northeast India. *Hum. Dimens. Wildl.* **9**, 261–270 (2004).
14. A. Sarker, E. Røskaft, Human attitudes towards the conservation of protected areas: A case study from four protected areas in Bangladesh. *Oryx* **45**, 391–400 (2011).
15. B. R. Tripathy *et al.*, Descriptive spatial analysis of human-elephant conflict (HEC) distribution and mapping HEC hotspots in Keonjhar forest division, India. *Front. Ecol. Evol.* **9**, 640624 (2021).
16. C. Williams *et al.*, Data from "Elephas maximus. The IUCN red list of threatened species." Available at https://dx.doi.org/10.2305/IUCN.UK.2020-3.RLTS.T7140A45818198.en. Retrieved 12-21. Deposited 18 September 2019.
17. K. S. Gobush *et al.*, Data from "Loxodonta africana. The IUCN Red List of threatened species." Available at https://dx.doi.org/10.2305/IUCN.UK.2021-1.RLTS.T181007989A204404464.en. Deposited 13 November 2020.
18. N. Seoraj-Pillai, N. Pillay, A meta-analysis of human-wildlife conflict: South African and global perspectives. *Sustainability* **9**, 34 (2016).
19. E. Di Minin, R. Slotow, C. Fink, H. Bauer, C. Packer, A pan-African spatial assessment of human conflicts with lions and elephants. *Nat. Commun.* **12**, 2978 (2021).
20. J. Wall *et al.*, Human footprint and protected areas shape elephant range across Africa. *Curr. Biol.* **31**, 2437–2445.e4 (2021).
21. S. de Silva *et al.*, Land-use change is associated with multi-century loss of elephant ecosystems in Asia. *Sci. Rep.* **13**, 5996 (2023).
22. R. Kanagaraj *et al.*, Predicting range shifts of Asian elephants under global change. *Divers. Distrib.* **25**, 822–838 (2019).
23. S. W. Dejene, K. S. Mpakairi, R. Kanagaraj, Y. A. Wato, S. Mengistu, Modelling continental range shift of the African elephant (*Loxodonta africana*) under a changing climate and land cover: Implications for future conservation of the species. *African Zool.* **56**, 25–34 (2021).
24. D. Schüßler, P. C. Lee, R. Stadtmann, Analyzing land use change to identify migration corridors of African elephants (*Loxodonta africana*) in the Kenyan-Tanzanian borderlands. *Landscape Ecol.* **33**, 2121–2136 (2018).
25. J. Anuradha, M. Fujimura, T. Inaoka, N. Sakai, The role of agricultural land use pattern dynamics on elephant habitat depletion and human–elephant conflict in Sri Lanka. *Sustainability* **11**, 2818 (2019).
26. S. Prabhakar, A succinct review and analysis of drivers and impacts of agricultural land transformations in Asia. *Land Use Policy* **102**, 105238 (2021).
27. M. DePaul, Climate change, migration, and megacities: Addressing the dual stresses of mass urbanization and climate vulnerability. *Paterson Rev. Int. Affairs* **12**, 145–162 (2012).
28. P. Dhanya *et al.*, Farmers' perceptions of climate change and the proposed agriculture adaptation strategies in a semi-arid region of South India. *J. Integrat. Environ. Sci.* **13**, 1–18 (2016).
29. H. Dagdeviren, A. Elangovan, R. Parimalavalli, Climate change, monsoon failures and inequality of impacts in South India. *J. Environ. Manag.* **299**, 113555 (2021).
30. S. J. Phillips, M. Dudík, R. E. Schapire, "A maximum entropy approach to species distribution modeling" in *Proceedings of the Twenty-first International Conference on Machine Learning* (2004), p. 83.
31. S. J. Phillips, R. P. Anderson, R. E. Schapire, Maximum entropy modeling of species geographic distributions. *Ecol. Modell.* **190**, 231–259 (2006).
32. S. Gubbi, Patterns and correlates of human–elephant conflict around a South Indian reserve. *Biol. Conserv.* **148**, 88–95 (2012).
33. K. K. Karanth, A. M. Gopalaswamy, P. K. Prasad, S. Dasgupta, Patterns of human–wildlife conflicts and compensation: Insights from Western Ghats protected areas. *Biol. Conserv.* **166**, 175–185 (2013).
34. D. Naha, S. Sathyakumar, S. Dash, A. Chettri, G. Rawat, Assessment and prediction of spatial patterns of human-elephant conflicts in changing land cover scenarios of a human-dominated landscape in North Bengal. *PLoS One* **14**, e0210580 (2019).
35. P. Sharma *et al.*, Mapping human–wildlife conflict hotspots in a transboundary landscape, Eastern Himalaya. *Global Ecol. Conserv.* **24**, e01284 (2020).
36. K. Riahi *et al.*, The shared socioeconomic pathways and their energy, land use, and greenhouse gas emissions implications: An overview. *Global Environ. Change* **42**, 153–168 (2017).
37. N. W. Sitati, M. J. Walpole, R. J. Smith, N. Leader-Williams, Predicting spatial aspects of human–elephant conflict. *J. Appl. Ecol.* **40**, 667–677 (2003).
38. N. Mmbaga, Human population growth as an indicator for human-elephant conflicts in Rombo area, Tanzania. *J. Biodivers. Environ. Sci.* **10**, 94–102 (2017).
39. P. K. Rawat, B. Pant, K. K. Pant, P. Pant, Geospatial analysis of alarmingly increasing human-wildlife conflicts in Jim Corbett National Park's Ramnagar buffer zone: Ecological and socioeconomic perspectives. *Int. J. Geoheritage Parks* **10**, 337–350 (2022).

40. M. D. Graham, B. Notter, W. M. Adams, P. C. Lee, T. N. Ochieng, Patterns of crop-raiding by elephants, *Loxodonta africana*, in Laikipia, Kenya, and the management of human–elephant conflict. *Systemat. Biodiver.* **8**, 435–445 (2010).
41. S. Wilson, T. E. Davies, N. Hazarika, A. Zimmermann, Understanding spatial and temporal patterns of human–elephant conflict in Assam, India. *Oryx* **49**, 140–149 (2015).
42. B. C. O'Neill *et al.*, The scenario model intercomparison project (scenariomip) for cmip6. *Geosci. Model Dev.* **9**, 3461–3482 (2016).
43. R. Sukumar, Ecology of the Asian elephant in southern India. II. Feeding habits and crop raiding patterns. *J. Trop. Ecol.* **6**, 33–53 (1990).
44. R. A. Pozo, T. Coulson, G. McCulloch, A. L. Stronza, A. C. Songhurst, Determining baselines for human-elephant conflict: A matter of time. *PLoS One* **12**, e0178840 (2017).
45. J. A. de la Torre *et al.*, There will be conflict–agricultural landscapes are prime, rather than marginal, habitats for Asian elephants. *Anim. Conserv.* **24**, 720–732 (2021).
46. N. Kitratporn, W. Takeuchi, Human-elephant conflict risk assessment under coupled climatic and anthropogenic changes in Thailand. *Sci. Total Environ.* **834**, 155174 (2022).
47. L. T. Ntukey, L. K. Munishi, E. Kohi, A. C. Treydte, Land use/cover change reduces elephant habitat suitability in the Wami Mbiki-Saadani Wildlife Corridor, Tanzania. *Land* **11**, 307 (2022).
48. M. M. Okello, S. J. Njumbi, J. W. Kiringe, J. Isiiche, Prevalence and severity of current human-elephant conflicts in Amboseli Ecosystem, Kenya: Insights from the field and key informants. *Nat. Res.* **5**, 462–477 (2014).
49. N. K. Nath *et al.*, An assessment of human-elephant conflict in Manas National Park, Assam, India. *J. Threatened Taxa* **1**, 309–316 (2009).
50. C. Santiapillai *et al.*, An assessment of the human-elephant conflict in Sri Lanka. *Ceylon J. Sci. (Biol. Sci.)* **39**, 21–33 (2010).
51. D. Neupane, R. L. Johnson, T. S. Risch, How do land-use practices affect human–elephant conflict in Nepal? *Wildlife Biol.* **2017**, 1–9 (2017).
52. E. M. Gross *et al.*, Seasonality, crop type and crop phenology influence crop damage by wildlife herbivores in Africa and Asia. *Biodivers. Conserv.* **27**, 2029–2050 (2018).
53. B. Neupane, S. Budhathoki, B. Khatiwoda, Human-elephant conflict and mitigation measures in Jhapa district, Nepal. *J. Forest Livelihood* **16**, 103–112 (2018).
54. J. M. Mukeka, J. O. Ogutu, E. Kanga, E. Røskaft, Human-wildlife conflicts and their correlates in Narok County, Kenya. *Global Ecol. Conservation* **18**, e00620 (2019).
55. R. Hoare, African elephants and humans in conflict: The outlook for coexistence. *Oryx* **34**, 34–38 (2000).
56. V. R. Goswami, K. Medhi, J. D. Nichols, M. K. Oli, Mechanistic understanding of human–wildlife conflict through a novel application of dynamic occupancy models. *Conserv. Biol.* **29**, 1100–1110 (2015).
57. B. R. Lamichhane *et al.*, Using interviews and biological sign surveys to infer seasonal use of forested and agricultural portions of a human-dominated landscape by Asian elephants in Nepal. *Ethol. Ecol. Evol.* **30**, 331–347 (2018).
58. V. Krishnan, M. A. Kumar, G. Raghunathan, S. Vijayakrishnan, Distribution and habitat use by Asian elephants (*Elephas maximus*) in a coffee-dominated landscape of southern India. *Trop. Conserv. Sci.* **12**, 1940082918822599 (2019).
59. O. Saif, R. Kansky, A. Palash, M. Kidd, A. T. Knight, Costs of coexistence: Understanding the drivers of tolerance towards Asian elephants (*Elephas maximus*) in rural Bangladesh. *Oryx* **54**, 603–611 (2020).
60. B. C. Borah, A. Bhattacharya, P. Sarkar, P. Choudhury, People's perception of human-elephant conflict in Rani–Garbhanga Reserve Forest of Assam, India. *GeoJournal* **87**, 4127–4141 (2022).
61. R. Kansky, M. Kidd, J. Fischer, Understanding drivers of human tolerance towards mammals in a mixed-use transfrontier conservation area in southern Africa. *Biol. Conserv.* **254**, 108947 (2021).
62. T. Thekaekara, S. A. Bhagwat, T. F. Thornton, Coexistence and culture: Understanding human diversity and tolerance in human-elephant interactions. *Front. Conserv. Sci.* **2**, 735929 (2021).
63. P. Virtanen *et al.*, Assessing tolerance for wildlife: Human–elephant conflict in Chimanimani, Mozambique. *Hum. Dimens. Wildl.* **26**, 411–428 (2021).
64. H. Jolly, T. Satterfield, M. Kandlikar, S. Tr, Indigenous insights on human-wildlife coexistence in southern India. *Conserv. Biol.* **36**, e13981 (2022).
65. M. Chen *et al.*, Global land use for 2015–2100 at 0.05 resolution under diverse socioeconomic and climate scenarios. *Sci. Data* **7**, 320 (2020).
66. A. J. Tatem, Worldpop, open data for spatial demography. *Sci. Data* **4**, 1–4 (2017).
67. M. Li *et al.*, Spatiotemporal dynamics of global population and heat exposure (2020–2100): Based on improved ssp-consistent population projections. *Environ. Res. Lett.* **17**, 094007 (2022).
68. J. Salerno *et al.*, Wildlife impacts and vulnerable livelihoods in a transfrontier conservation landscape. *Conserv. Biol.* **34**, 891–902 (2020).
69. A. K. Ram *et al.*, Patterns and determinants of elephant attacks on humans in Nepal. *Ecol. Evol.* **11**, 11639–11650 (2021).
70. UNEP-WCMC and IUCN, Data from "Protected Planet: The World Database on Protected Areas (WDPA)" Available at: https://www.protectedplanet.net. Deposited 1 December 2022.
71. S. Chamberlain, D. Oldoni, J. Waller, Data from "rgbif: Interface to the Global BiodiversityInformation Facility API." Zenodo. Available at https://doi.org/10.5281/zenodo.6023735. Deposited 9 February 2022.
72. J. Shoshani, J. F. Eisenberg, *Elephas maximus*. *Mamm. Species* **182**, 1–8 (1982).
73. R. C. Fleischer, E. A. Perry, K. Muralidharan, E. E. Stevens, C. M. Wemmer, Phylogeography of the Asian elephant (*Elephas maximus*) based on mitochondrial DNA. *Evolution* **55**, 1882–1892 (2001).
74. D. N. Karger *et al.*, Climatologies at high resolution for the Earth's land surface areas. *Sci. Data* **4**, 1–20 (2017).
75. M. Alamgir, S. A. Mukul, S. M. Turton, Modelling spatial distribution of critically endangered Asian elephant and hoolock gibbon in Bangladesh forest ecosystems under a changing climate. *Appl. Geography* **60**, 10–19 (2015).
76. J. M. Kass *et al.*, Wallace: A flexible platform for reproducible modeling of species niches and distributions built for community expansion. *Methods Ecol. Evol.* **9**, 1151–1156 (2018).
77. O. M. Richmond, J. P. McEntee, R. J. Hijmans, J. S. Brashares, Is the climate right for Pleistocene rewilding? Using species distribution models to extrapolate climatic suitability for mammals across continents. *PLoS One* **5**, e12899 (2010).
78. M. Guarnieri *et al.*, Code and data from "Effects of climate, land use, and human population change on human–elephant conflict risk in Africa and Asia." Github. https://github.com/gkumaishi/Elephant_HWC. Deposited 18 December 2023.